Uniform Ultrasmall Manganese Monoxide Nanoparticle/Carbon Nanocomposite as a High-Performance Anode for Lithium Storage

Ting Wang[a,b], Xiaolong Zhang[a], Fan Zhang[a], Wenlou Wang[b], Yan Liang[a], Yongbing Tang[a,*]

[a] Functional Thin Films Research Center, Shenzhen Institutes of Advanced Technology, Chinese Academy of Sciences, Shenzhen 518055, China
[b] Nano Science and Technology Institute, University of Science and Technology of China, Suzhou 215123, China

ARTICLE INFO

ABSTRACT

In this study, uniformly dispersed MnO@C nanocomposite with an average MnO particle size of 10 nm is synthesized via a simple wet-chemical/carbonization method. In the MnO@C nanocomposite, ultrasmall MnO nanoparticles are homogeneously coated with carbon layers. As an anode material for lithium ion batteries (LIBs), this nanocomposite shows significantly enhanced electrochemical performances compared with the non-carbon coated material due to the conductive carbon layer, which provides an ideal conductive matrix for electron/ion transfer and a buffer layer to accommodate the MnO expansion during lithiation process. As a result, the MnO@C nanocomposite exhibits a high reversible capacity of $\sim$750 mAh/g over 600 cycles at a current density of 0.7 A/g and a high-rate capability of $\sim$340 mAh/g even at 2.1 A/g, which are among the best reported electrochemical performances for MnO-based materials thus far, demonstrating its potential application in LIBs with long cycling life and high power density.

© 2016 Elsevier Ltd. All rights reserved.

1. Introduction

Lithium ion batteries (LIBs) with high electricity storage capacity and long cycling stability are of great importance for the increasing demands from mobile electronic devices to electric vehicles [1,2]. However, the limited capacity (372 mAh/g) of the conventional anode material (i.e. graphite) is not sufficient for the next generation energy storage system [3,4]. Therefore, a key challenge of developing next generation LIBs is to find alternative anode materials with higher lithium storage capacity. Extensive efforts have been devoted to develop new anode materials, such as transition metal oxides [5–11], transition metal sulfides [12–14], silicon-based [15–20] and tin-based materials [21–24]. Among them, manganese oxides have attracted much attention for their high theoretical specific capacities (755–1232 mAh/g) and natural abundance [25–29].

However, like other transition metal oxides, the electrochemical performances of manganese oxides are hindered by their low electrical conductivity and large volume expansion during charge/discharge process. One strategy to address this problem is constructing manganese oxides with unique microstructure to shorten the diffusion length of Li$^+$ and accommodate the volume change during charge/discharge process, such as downsizing the manganese oxides into nanoscale with special morphologies [30–33] and engineering hollow or porous structures [34–37]. Another strategy is combining manganese oxides with other high conductivity materials, such as carbon nanotubes [38–41], graphene [25,42–45] and other carbon materials [46–50]. It has been pointed out that encapsulating or coating manganese oxides with carbon layers is an effective approach to optimize their electrochemical performances [46,48,51–54]. However, most of carbon coated manganese oxides nanostructures suffer from intensive aggregation problem, which is unsuitable for sufficient electrochemical reactions [31,55–57].

In this study, a MnO@C nanocomposite with ultrasmall MnO nanoparticles uniformly coated with carbon layers was synthesized via a simple wet-chemical/carbonization method. Owing to the introduction of conductive carbon layer, which provides an ideal conductive matrix for electron/ion transfer and a buffer layer to accommodate the MnO expansion during lithiation process, the MnO@C nanocomposite exhibits significantly improved LIB electrochemical performances, which delivers a reversible capacity of $\sim$750 mAh/g over 600 cycles at 0.7 A/g, and a high-rate

---

* Corresponding author.
E-mail address: tangyb@siat.ac.cn (Y. Tang).

capability of ~340 mAh/g even at 2.1 A/g, among the best reported electrochemical performances for MnO-based materials thus far.

2. Experimental

2.1. Materials synthesis

2.1.1. Synthesis of MnO_2 nanosheets

Scheme 1 illustrates the process of MnO_2, Mn_2O_3 and MnO@C nanocomposites. MnO_2 nanosheets as the precursor were synthesized by a facile one-step wet chemical method. In detail, 10 g Mn$(CH_3COO)_2 \cdot 4H_2O$ was ultrasonically dissolved into 200 ml ethylene glycol, and 10 g $(NH_4)_2S_2O_8$ was dissolved in 200 ml H_2O. The two solutions were mixed together thoroughly and stirred for 1 min. Then, the reaction system stood in a water bath at 50 °C for 1 h. Finally, the dark brown suspended solids were filtrated and dried at 60 °C overnight.

2.1.2. Synthesis of MnO@C nanocomposites

The MnO_2 was annealed in a muffle furnace for 1 h under air atmosphere at 600 °C to obtain Mn_2O_3 monodispersed nanoparticles. Then, 0.4 g of the as-obtained Mn_2O_3 nanoparticles were dispersed in 70 ml distilled water and magnetically stirred at room temperature, followed by adding 1.5 ml PEG-400 and 1.5 mmol ascorbic acid to form a suspension. After stirring for 5 minutes, the suspension was heated to 95 °C to evaporate the water. Subsequently, the resulting mixture was kept at 500 °C for 6 h in a tube furnace under the protection of Ar to obtain MnO@C nanocomposites.

2.2. Materials characterization

The phase purity and crystalline structure of the as-prepared MnO_2, Mn_2O_3 and MnO@C nanocomposites were detected by X-ray diffraction (XRD, Rigaku TTR-III with Cu Kα radiation) operated at 40 kV × 100 mA and over a 2Θ degree ranged from 10° to 80°. The morphologies and nanostructures were examined by field-emission scanning electron microscopy (FE-SEM, FEI Nova Nano-SEM 450) and transmission electron microscopy (TEM, FEI Tecnai G^2 F30). To evaluate the carbon content and the phase transition of the products, thermogravimetric analysis (TGA SDT Q600) was performed in air atmosphere from room temperature to 800 °C at a heating rate of 10 °C/min.

2.3. Electrochemical measurements

Acetylene black and polyvinylidene fluoride (PVDF) were mixed with active materials by a weight ratio of active material: acetylene black: PVDF = 8: 1: 1 in N-methyl-2-pyrrolidone (NMP). The obtained slurry was then pasted on Cu foil and kept in vacuum oven at 120 °C for 12 h. The loading mass of active material was approximately 1.20 mg/cm^2 and its electrochemical performance was evaluated by CR2032 coin cells. Li metal was used as counter electrode, and 1 M LiPF$_6$ in ethylene carbonate, diethyl carbonate and ethyl methyl carbonate (EC: DEC: EMC = 1: 1: 1 v/v/v) was used as electrolyte. The coin cells were assembled in an argon filled glove box (Etelux Lab2000), and the charge/discharge tests were operated by a LAND-battery cycler (Wuhan, China) in a voltage range from 0.02 V to 3.0 V. Cyclic voltammetry (CV) at a scan rate of 0.2 mV/s and electrochemical impedance spectroscopy (EIS) from 0.1 Hz to 100000 Hz were conducted by an electrochemical workstation (Autolab PGSTAT302N).

3. Results and discussion

3.1. Composition and morphology

Fig. 1 shows the XRD patterns of MnO_2, Mn_2O_3, and MnO@C. The diffraction pattern of MnO_2 is in consistent with α-phase MnO_2 intermediate as reported in previous study [58]. The wide weak bands indicate the high disorder and low crystallinity of the MnO_2 precursor [59]. After annealing at 600 °C, MnO_2 converted to bixbyite-C Mn_2O_3 (pdf No. 41-1442) as shown in the XRD pattern (blue line). The XRD pattern of the MnO@C nanocomposite is indexed to characteristic diffraction peaks of manganosite MnO (pdf No. 07-0230) instead of Mn_2O_3, indicating a reduction function of the coated carbon layer. However, no characteristic peaks of carbon can be observed, which is possibly because the carbon is amorphous or the content of crystalline carbon is too low to be detected.

To determine the carbon content in the MnO@C nanocomposite, TG analysis was carried out under air atmosphere, as presented in Fig. 2. As both MnO and carbon involve in certain chemical changes during the heating process, the TG curve shows complicated weight change. The initial small weight loss below 150 °C is caused by the evaporation of surface absorbed water. Between 150 and 260 °C, there is a weight increase which may be caused by the partial phase transition of MnO to MnO_2. The subsequent weight loss in the temperature range of 260 to 530 °C is ascribed to the combustion of carbon component which is about 7.56 wt% and the reduction of MnO_2 to MnO. From 540 to 600 °C, the weight increase is supposed to be associated with the oxidation of manganese oxides [55].

The morphologies and nanostructures of MnO_2, Mn_2O_3, and MnO@C were characterized by SEM and TEM (Fig. 3). As shown in
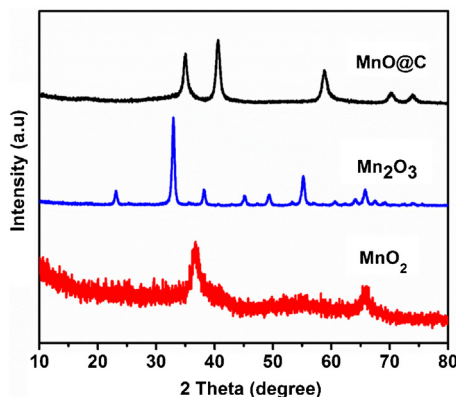

Fig. 1. XRD patterns of MnO_2 (red line), Mn_2O_3 (blue line), and MnO@C (black line). (For interpretation of the references to colour in this figure legend, the reader is referred to the web version of this article.)